A Genome-wide Linkage Analysis and Mutation Analysis of Hereditary Congenital Blepharoptosis in a Japanese Family

Mitsuko Nakashima[1,2], Motoi Nakano[2], Akiyoshi Hirano[2], Tatsuya Kishino[3,5], Shinji Kondoh[3,5], Nobutomo Miwa[1,5], Norio Niikawa[4,5], Koh-ichiro Yoshiura[1,5]

[1]Department of Human Genetics and [2]Division of Plastic and Reconstructive Surgery, Nagasaki University Graduate School of Biomedical Sciences, Nagasaki, Japan; [3]Division of Functional Genomics, Center for Frontier Life Sciences, Nagasaki University, Nagasaki, Japan; [4]The Research Institute of Personalized Health Sciences, Health Sciences University of Hokkaido, Hokkaido, Japan; [5]Solution Oriented Research for Science and Technology (SORST), Japan Science and Technology Agency (JST), Tokyo, Japan.

Correspondence to Dr. Koh-ichiro Yoshiura, Department of Human Genetics, Nagasaki University Graduate School of Biomedical Sciences, Sakamoto 1-12-4, Nagasaki 852-8523, Japan.
TEL: +81-95-849-7120; FAX: +81-95-849-7121; e-mail: kyoshi@nagasaki-u.ac.jp

ABSTRACT

Hereditary congenital ptosis (PTOS) is defined as drooping of the upper eyelid without any other accompanying symptoms and distinguished from syndromic blepharoptosis. Two previous linkage analyses assigned a PTOS locus (PTOS1) to 1p32-p34.1 and another (PTOS2) to Xq24-q27.1. In addition, in a sporadic case with a balanced chromosomal translocation t(1;8)(p34.3;q21.12), the *ZFHX4* (zinc finger homeodomain 4) gene was found to be disrupted at the 8q21.12 breakpoint, but there was no gene at the 1p34.3 breakpoint, suggesting the existence of the third PTOS locus (PTOS1) at 8q21.12. We carried out a genome-wide linkage analysis in a Japanese PTOS family and calculated two-point and multipoint LOD scores with reduced penetrance. Haplotype analysis gave three candidate disease-responsible regions, i.e., 8q21.11-q22.1, 12q24.32-q24.33 and 14q21.1-q23.2. Although the family size is too small to define one of them, 8q21.11-q22.1 is a likely candidate region, because it contains the previously reported translocation breakpoint above. We thus performed mutation, Southern-blot and methylation analyses of *ZFHX4*, but could not find any disease specific change in the family. Nevertheless, our data may support the localization of PTOS1.

Key words: Hereditary congenital ptosis; *ZFHX4*

INTRODUCTION

Blepharoptosis is pathological drooping of the upper eyelid. It is classified into myogenic, neurogenic, aponeurotic and mechanical ptosis, according to the primarily affected lesion. Hereditary congenital ptosis (PTOS) distinguished from other syndromic blepharoptosis involves only the upper eyelid. PTOS is genetically heterogeneous and two modes of inheritance have been known: autosomal dominant PTOS1 (MIM %178300) and X-linked PTOS2 (MIM %300245). Autosomal PTOS may be further devided into at least two types. Engle et al. (1997) mapped PTOS1 by linkage analysis to 1p32-p34.1, while McMullan et al. (2002) found, by the analysis of a sporadic case of PTOS who had a *de novo* balanced chromosomal translocation t(1;8)(p34.3;q21.12), that the *ZFHX4* gene at 8q21.12 was disrupted by the translocation but there was no gene at the 1p34.3 breakpoint, suggesting the third locus at 8q21.12.

We recently encountered a Japanese family with PTOS in which there are nine affected members in five successive generations. Here we report on a linkage analysis and mutation analysis of a candidate gene, *ZFHX4*.

MATERIALS AND METHODS

Family and Patients

A Japanese family consisted of at least nine members affected with PTOS in five generations (Fig. 1). The disease in the family was found in both sexes and transmitted (male to male transmissions twice) directly through successive generations, indicatng that it is autosomal dominant PTOS. A total of 18 members including five affected and 12 non-affected members, and one of their spouses participated in this study. The proposita (V-5, Figs. 1 and 2) suffered from congenital ptosis on her right eye, and visited Department of Plastic and Reconstructive Surgery, Nagasaki University Hospital at age 15 years. She had severe ptosis (drooping > 4 mm, levator function = 5 mm) without any other ophthalmic disorders and appeared to have overaction of the frontalis muscle. She had undergone a levator muscle shortening surgery for her ptosis. Three patients (III-13, IV-2 and IV-12) suffered from unilateral congenital ptosis and all had undergone a repair surgery. The other patient (III-5) with bilateral ptosis has received no surgical treatment. None of

the five patients had any associated ophthalmic disorders and all were examined by one or two well-trained plastic surgeons. The study protocol was approved by the Committee for the Ethical Issues on Human Genome and Gene Analysis in Nagasaki University.

Linkage and Haplotype Analyses

After obtaining written informed consent from each participant, DNA was extracted by conventional method from their whole blood, or using ISOHAIR^{TM} (Nippon Gene, Tokyo, Japan) from their fingernail clippings, concentrated, and then purified by phenol-chloroform method (Matsuzawa et al. 2006) For whole-genome scanning, we used ABI Prism Linkage Mapping Set-MD10 (AppliedBiosystems, Foster City, CA, USA) that consists of 386 microsatellite markers from whole chromosomes with average distance of about 10 cM. Polymerase chain reaction (PCR) was performed in a 10 μl mixture containing 5 ng genomic DNA/0.25 U ExTaq DNA polymerase HS-version (TAKARA Bio Inc., Kyoto, Japan)/200 μM dNTP/0.3 μM primer/1xPCR buffer on the Dual 384-well GeneAmp PCR System 9700 Thermal Cycler (AppliedBiosystems). The PCR condition was composed of initial denaturation at 94 °C for 3 min, followed by 37 (blood samples) or 44 (nail samples) cycles of amplification at 94 °C, 30 sec/55 °C, 30 sec/72 °C, 30 sec, and final extension at 72 °C for 7 min. PCR products were analysed on an Autosequencer Model 3100. Genotyping was carried out using GeneScan and Genotyper software (AppliedBiosystems).

Two-point LOD score was calculated using MLINK program (included in FASTLINK software version 4.0P) (Lathrop et al. 1984), and multipoint LOD score and nonparametric LOD score were calculated using Genehunter software (Kruglyak et al. 1996). To pick up all possibly linked loci, calculation was based on an assumption that the ptosis in the family is an autosomal dominant trait with 90% penetrance (p=0.9) and on the allele frequency of 1/N, where the number of alleles is N. Haplotypes around loci with positive LOD scores were constructed with 4 or 5 microsatellite markers that were set up at intervals of 2-3 cM. Information of these microsatellite markers was referred to the NCBI database (Map Viewer: Marshfield and/or decode map).

Mutation Analysis

ZFHX4 reported to have been disrupted by a translocation in a patient with PTOS (McMullan et al. 2002) is located at 8q21.1. As its chromosomal localization is one of candidate regions we identified in the present study, we performed direct sequencing of all exons of *ZFHX4* using DNA from one affected member (III-5) and one unaffected member (IV-1) in the family. The genomic sequence of *ZFHX4* was retrieved from the UCSC Genome Browser Home (http://genome.ucsc.edu/) and from the Ensemble Genome Browser (http://ensembl.org/index.html). Primers were designed from sequences of each exon and those around respective intron. PCR was performed in a 15 μl reaction mixture containing 5 ng DNA/0.4 U ExTaq DNA polymerase/200 μM dNTP/0.67 μM each primer/1xPCR buffer on DNA Thermal Cycler Model 9700 (AppliedBiosystems) with a condition of initial denaturation at 94 °C for 3 min, amplification for 37 cycles at 94 °C, 30sec/60 °C, 30 sec/72 °C, 30-60 sec, and final extension at 72 °C for 7 min. PCR products were subjected to cleaning-up using Exonuclease I (Epicentre, WI, USA) and shrimp alkaline phosphatase (AmershamBioscience, NJ, USA) for direct sequence reaction. Direct sequencing was carried out using BigDye-terminator sequencing reagent version-3.1 (AppliedBiosystems) on an Autosequencer Model 3100, and sequences were aligned with ATGC software (GENETYX Corp., Tokyo, Japan).

Southern Blot Analysis

Genomic DNA from a patient (III-5) as a representative from the family was digested with three different enzymes (*Bam*HI, *Eco*RI, *Hin*dIII) and electrophoresed on 0.8% agarose gel in 0.5xTBE buffer containing 0.25 μg/ml ethidium bromide at 35~40 volts for 6-10 hrs. DNA was then denatured with 0.4 N NaOH for 15-20 min and capillary-transferred overnight onto nylon membrane (HybondN+, AmershamPharmacia Biotech, Buckinghamshire, UK) using alkaline transfer buffer, and the membrane was washed twice with 2xSSC. DNA fixed to the membrane by UV cross-linking was hybridized to fluorescein-labeled probes using Gene Images Random Prime Labeling Kit (AmershamBiosciences). Hybridized signal was detected using Gene Image CDP-Star Detection Kit (AmershamBiosciences). Genomic DNA from phenotypically normal

individuals were used as controls.

Methylation Analysis of *ZFHX4*

DNA (1 μg) from patients and a control individual was modified with sodium bisulfite using CpGenome DNA modification Kit (CHEMICON, CA, USA). PCR primers specific for methylated or unmethylated DNA (Herman et al. 1996) were desinged from sequences of two CpG islands of *ZFHX4* (Table 1) at which one island is located 3-kb upstream and the other 0.4-kb downstream of exon 1, espectively (Hemmi et al. 2006). Methylation-specific PCR was performed in a 20 μl reaction mixture containing 50 ng bisulfite-modified DNA/0.5 U AmpliTaq Gold (AppliedBiosystems)/200 μM dNTP/0.5 μM each primer/1xPCR buffer with a condition consisting of initial denaturation at 95 °C for 10 min, 37 cycles of amiplification at 94 °C, 30 sec/60 °C, 30 sec/72 °C, 30 sec, and final extension at 72 °C for 10 min. PCR products were analyzed by electrophoresis on 2.5% agarose gel. Because aberrant signals on Southern blot were observed, the bisulfite-modified DNA was also amplified with specific primers for *Eco*RI site around exon12 of *ZFHX4*. PCR products were cloned using TOPO TA cloning Kit (Invitrogen, Carlsbad, CA, USA), and then cloned DNA was sequenced (Clark et al. 1994).

RESULTS

Linkage and Haplotype Analyses

As the number of affected members in this family was small and penetrance might be considerably low, we set a cut-off LOD score ≥ 0.4 in all calculations. The two-point and multi-point analyses gave nine markers (D1S255, D1S484, D5S630, D7S669, D9S1776, D11S4046, D19S221, D19S226, and D14S276) that show such scores, and the non-prametric analysis gave four candidate regions (3q22.1, 8q21.11, 12q24.32, and 20p13). The haplotype analysis at these loci revealed that all but 8q21.1, 12q24.3 and 14q22.3 regions (Fig. 1) were excluded, because some patients do not have putative disease-linked haplotypes (data not shown). Thus, we finally left these three regions commonly shared by the patients as candidates. Further refinement was impossible, because any more family samples were not available.

Mutation Analysis of the *ZFHX4* Gene

The direct sequencing of *ZFHX4* revealed one missense alteration (G12411T or L4137F) in exon12 in the affected member and some normal control samples (data not shown), indicating that it is actually a single nucleotide polymorphism (SNP). Likewise, another mutation analysis for homologous sequences between the mouse and human in their promotor/enhancer region of *ZFHX4/Zfhx4* revealed no disease-associated mutation in the patient. Southern blot analysis using a probe for exon 2 or exon 12 of *ZFHX4* detected an respective extra *Eco*RI-fragment in a patient (III-5) (Fig. 3), and an extra band for exon 12 also in two other patients (III-13 and IV-12), while there were no aberrant signals with other restriction enzymes. However, sequence analysis of these regions did not identify any genomic rearrangements, and confirmed no RFLP around exon 2 or 12. These led us to try to detect the differential methylation status in the regions between patients and normal controls. However, methylation-specific PCR following a bisulfite treatment revealed no change of the methylation status in the patient's two CpG-islands (data not shown).

DISCUSSION

In this study, we performed linkage and haplotype analyses of a Japanese PTOS pedigree. Consequently, three regions, 8q21.11-q22.2, 12q24.32-qter and 14q21.1-q23.2, were shown to be candidates. The two-point maximum LOD scores were considerably low, being 1.16, 0.47 and 0.72 at *D8S551*, *D12S1659* and *D14S276* (Table 2), respectively, because some unaffected family members also had disease-linked haplotypes around the markers. It was obvious that the disease in the family shows incomplete penetrance. Although we diagnosed carefully many members of the family at the beginning of this study, we might have overlooked very mildly affected members.

Two regions responsible for autosomal PTOS were reported previously, i.e., 1p34.1-p32 for PTOS1 by linkage analysis (Engle et al. 1997) and 1p34.3/8q21.12 by analysis of a chromosomal translocation (McMullan et al. 2002). Three candidate loci we have detected include the translocation breakpoint, 8q21.2 (McMullan et al. 2002), but do not contain 1p34.1-p32 (Engle et al. 1997). Therefore, the disease locus for our family could

be associated with PTOS1. However, we failed to identify in our family any point mutation, genomic rearrangement or methylation aberration involving *ZFHX4* that was disrupted at the 8q21.12 breakpoint of the translocation in a PTOS patient (McMullan et al. 2002).

The human *ZFHX4* gene spans about 180-kb long, contains 12 exons, is mapped at 8q13.3-q21.11, and has >90% homology to the mouse *Zfh4* and 52% to the human *ATBF1* (Hemmi et al. 2006). The *Zfh4* gene encodes a member of the zincfinger-homeodomain family which has 4 homeodomains and 22 zinc fingers (Sakata et al. 2000). *Zfh4* was highly expressed in developing muscle and brains of the mouse, especially in the midbrain and hindbrain (Kostich and Sanes 1995), and was also detected in adult rat oculomotor nucleus which controls the levator palpebrae superioris (LPS) muscle (Nogami et al. 2005). The oculomotor nucleus exists in the mesencephalon. The oculomotor nerve innervates to LPS and the extraocular muscles except for the lateral rectus and the superior oblique muscle, and also supplies parasympathetic preganglionic fibers to the ciliary ganglion through which postganglionic nerve controls the ciliary muscle and the sphincter muscle of pupil. It was reported that *ZFHX4* was upregulated in postmitotic neurons and suggested that *ZFHX4* was influenced on neural differentiation including migration and axon out-growth (Nogami et al. 2005; Hemmi et al. 2006). All these lines of evidence strongly suggest that *ZFHX4* is the responsible gene for a type of PTOS.

There are two opinions concerning the pathological change in LPS from congenital ptosis. Three reports approved that congenital ptosis is caused by primary dysgenesis or myodystrophy of LPS (Berke and Wadsworth. 1955; Isaksson et al. 1961; 1962; Stula et al. 1988). On the other hand, Edmunds et al. (1998) argued against such a mechanism, because there was no significantly different histology between LPS from PTOS patients and normal individuals. A light-microscope study of an LPS specimen from the proband in our family showed that the muscle fibers were displaced by fibrous and fatty tissues and scanty atrophic striated muscles remained. This histological finding is consistent with dysgenesis of LPS. Therefore, if *ZFHX4* is relevant to congenital blepharoptosis, its abnormal expression might cause a failure of neuronal differentiation of the oculomotor nerve, leading to LPS dysgenesis.

In conclusion, we identified three possible regions candidate for PTOS1, 8q21.11-q22.2, 12q24.32-qter and 14q21.1-q23.2, by a whole-genome linkage analysis. These regions do not definitely overlap with a 1p34.1-p32 segment to which PTOS1 was mapped (Engle et al. 1997), and one of the regions we assigned includes a segment containing *ZFHX4* (McMullan et al. 2000). Thus, our data may support the existence of the PTOS1 locus. It remains to be seen whether other PTOS1 families have mutations in *ZFHX4*, another gene, or in a putative *ZFHX4* enhancer located at 8q21.11-q22.2.

ACKNOWLEDGEMENTS

We are indebted to the family members for their participation in this study. We especially thank N. Noguchi, A. Goto, and K. Miyazaki for their technical assistance. N. N. was supported in part by Grant-in-Aid for Scientific Research on Priority Areas (Applied Genomics, No. 17019055) from the Ministry of Education, Culture, Sports, Science and Technology (MEXT) of Japan, and by SORST from the Japan Science and Technology Agency (JST). K.Y. was supported by Grant-in-Aid for Scientific Research on Priority Areas (No. 17590288) from MEXT of Japan.

REFERENCES

Berke RN.; Wadsworth JAC (1955) Histology of levator muscle in congenital and acquired ptosis. Arch Opthalmol 53:413-428

Clark SJ, Harrison J, Paul CL, Frommer M (1994) High sensitivity mapping of methylated cytosines. Nucleic Acids Res 22:2990-2997

Edmunds B, Manners RM, Weller RO, Steart P, Collin JRO (1998) Levator palpebrae superioris fibre size in normals and patients with congenital ptosis. Eye 12:47-50

Engle EC, Castro AE, Macy ME, Knoll JH, Beggs AH (1997) A gene for isolated congenital ptosis maps to a 3-cM region within 1p32-p34.1. Am J Hum Genet 60:1150-1157

Hemmi K, Ma D, Miura Y, Kawaguchi M, Sasahara M, Tamaoki TH, Tamaoki T, Sakata N, Tsuchiya K (2006) A homeodomain-zinc finger protein, ZFHX4, is expressed in neuronal differentiation manner and suppressed in muscle differentiation manner. Biol Pharm Bull 29:1830-1835

Herman JG, Graff JR, Myöhänen S, Kelkin BD, Baylin B (1996) Methylation-specific PCR: A novel PCR assay for methylation status of CpG islands. Proc Natl Acad Sci 93:9821-9826

Isaksson I; Mellgren J (1961) Pathological-anatomical changes in the levator palpebrae superioris muscle in congenital ptosis. Acta Pathol Microbio Scand 144: 157-160

Isaksson I. Studies on congenital genuine blepharoptosis. 1962. Acta Opthalmol 72 (suppl) 1-120

Kostich WA, Sanes JR (1995) Expression of zfh-4, a member of the zinc finger-homeodomain family, in developing brain and muscles. Dev Dyn 202: 145-152

Kruglyal L, Daly MJ, Reeve-Daly MP, Lander ES (1996) Parametric and nonparametric linkage analysis: a unified multipoint approach. Am J Hum Genet 58:1347-63

Lathrop GM, Lalouel JM, Julier C, Ott J. 1984. Strategies for multilocus linkage analysis in humans. Proc Natl Acad Sci USA 81: 3443-3446

Matsuzawa N, Shimozato K, Natsume N, Niikawa N, Yoshiura K (2006) A novel missense mutation in Van der Woude syndrome: usefulness of fingernail DNA for genetic analysis.

J Dent Res 85:1143-1146

McMullan TFW, Crolla JA, Gregory SG, Carter NP, Cooper RA, Howell GR, Robinson DO (2002) A candidate gene for congenital bilateral isolated ptosis identified by molecular analysis of a de novo balanced translocation. Hum Genet 110:244-250

McMullan TFW, Tyers AG (2001) X linked dominant congenital isolated bilateral ptosis: the definition and characterisation of a new condition Brit J Opthalmol 85:70-73

Nogami S, Ishii Y, Kawaguchi M, Sakata M, Oya T, Takagawa K, Kanamori M, Sabit H, Obata T, Kimura T, Sasahara M (2005) ZFH4 protein is expressed in many neurons of developing rat brain. J Comp Neurol 482:33-49

Sakata N, Hemmi K, Kawaguchi M, Miura Y, Noguchi S, Ma D, Sasahara M, Hori M, Tamaoki T (2000) The Mouse ZFH-4 Protein Contains Four Homeodomains and Twenty-Two Zinc Fingers. Biochem Biophys Res Comm 273:686-693

Stula FC (1988) Histological changes in congenital and acquired blepharoptosis. Eye 2:179-184

Figure Legend

Figure 1. Family tree with haplotypes at (A) 8q21.11-q22.2, (B) 12q24.32-qter and (C) 14q21.1-q23.2 regions. Closed, open and slash symbols indicate affected, unaffected, and deceased individuals, respectively. Double horizontal line depicts consanguineous marriage, and short bar above individual symbols indicate individuals examined clinically. Thick columns depict disease-associated haplotypes.

Figure 2. Blepharopotosis of two affected members (V-5 and III-5). The proband (V-5) has unilateral blepharoptosis (**A**), and III-5 has bilateral ptosis (**B**). Both patients have overaction of the frontalis muscle.

Figure 3. Southern blot analysis of patients (P3) and a control individual (C) after digestion with three different enzymes, using probes for exons 2 and 12 of *ZFHX4*. An extra band is seen in *Eco*RI fragments including *ZFHX4* from a patient (III-5, P3) (**A**) and three patients (P1, III-13; P2, IV-12; and P3) (**B**).

Table.1 Polymerase chain reaction (PCR) primers for methylation-specific PCR and bisulfite sequencing

Primer	Sequences 5’ → 3’	Anneal temperature	Products size(bp)
CpG1-MF	GTTTAGTCGTTCGGATCGCGTTCGT	60	182
CpG1-MR	AACTTAACCTCGAAACGCGCCAACG		
CpG1-UF	GTTAGGTTTAGTTGTTTGGATTGTGTTTGT	60	192
CpG1-UR	TCCAAAACTTAACCTCAAAACACACCAACA		
CpG2-MF	GGGTTTTGTTTTTTTCGCGAGTTTC	60	139
CpG2-MR	TACGAAAAACCAATCATCCCAATCG		
CpG2-UF	TTTTTGGGTTTTGTTTTTTTTGTGAGTTTT	60	149
CpG2-UR	ATAAATACAAAAAACCAATCATCCCAATCA		
Ex12-upF	GGAAAGTAAAGAAGTTGTTTTAAAA	56	180
Ex12-upR	ATAACAAAACAATACAACACAAATA		
Ex12-dwF	TGATAATGGTAGAAGGTAAAGTATT	56	200
Ex12-dwR	AACATATAAAACAAAAAAACCTCTA		

M methylated-specific, *U* unmethylated-specific, *F* forward primer, *R* reverse primer, *up* upstream restriction site, *dw* downstream restriction site

Table.2 Log of odds (LOD) scores of candidate loci of the third hereditary congenital ptosis locus (PTOS1)

	Recombination Fraction (θ)						Multipoint
Locus	0.00	0.05	0.10	0.20	0.30	0.40	LOD score
D8S551	0.95	1.12	1.16	1.01	0.68	0.29	1.46
D8S525	0.15	0.12	0.09	0.05	0.02	0.00	1.51
D8S270	-2.53	-1.33	-0.86	-0.36	-0.13	-0.02	1.39
D8S1772	0.33	0.31	0.29	0.23	0.15	0.08	1.22
D12S1679	-0.03	0.31	0.45	0.47	0.34	0.17	0.59
D12S1659	0.15	0.12	0.09	0.05	0.02	0.00	1.39
D12S97	-0.20	-0.11	-0.05	-0.00	0.00	0.00	1.61
D12S1599	-0.78	-0.43	-0.27	-0.11	-0.04	-0.01	1.63
D12S1723	0.15	0.25	0.27	0.23	0.14	0.06	1.79
D14S1057	0.62	0.64	0.61	0.51	0.37	0.20	-1.00
D14S276	0.46	0.65	0.72	0.65	0.44	0.19	1.31
D14S66	-1.65	-1.15	-0.83	-0.45	-0.25	-0.12	2.01
D14S274	-1.16	-0.30	-0.07	0.07	0.07	0.02	1.97
D14S1038	-2.15	-1.64	-1.27	-0.76	-0.43	-0.19	1.94

Figure 1A

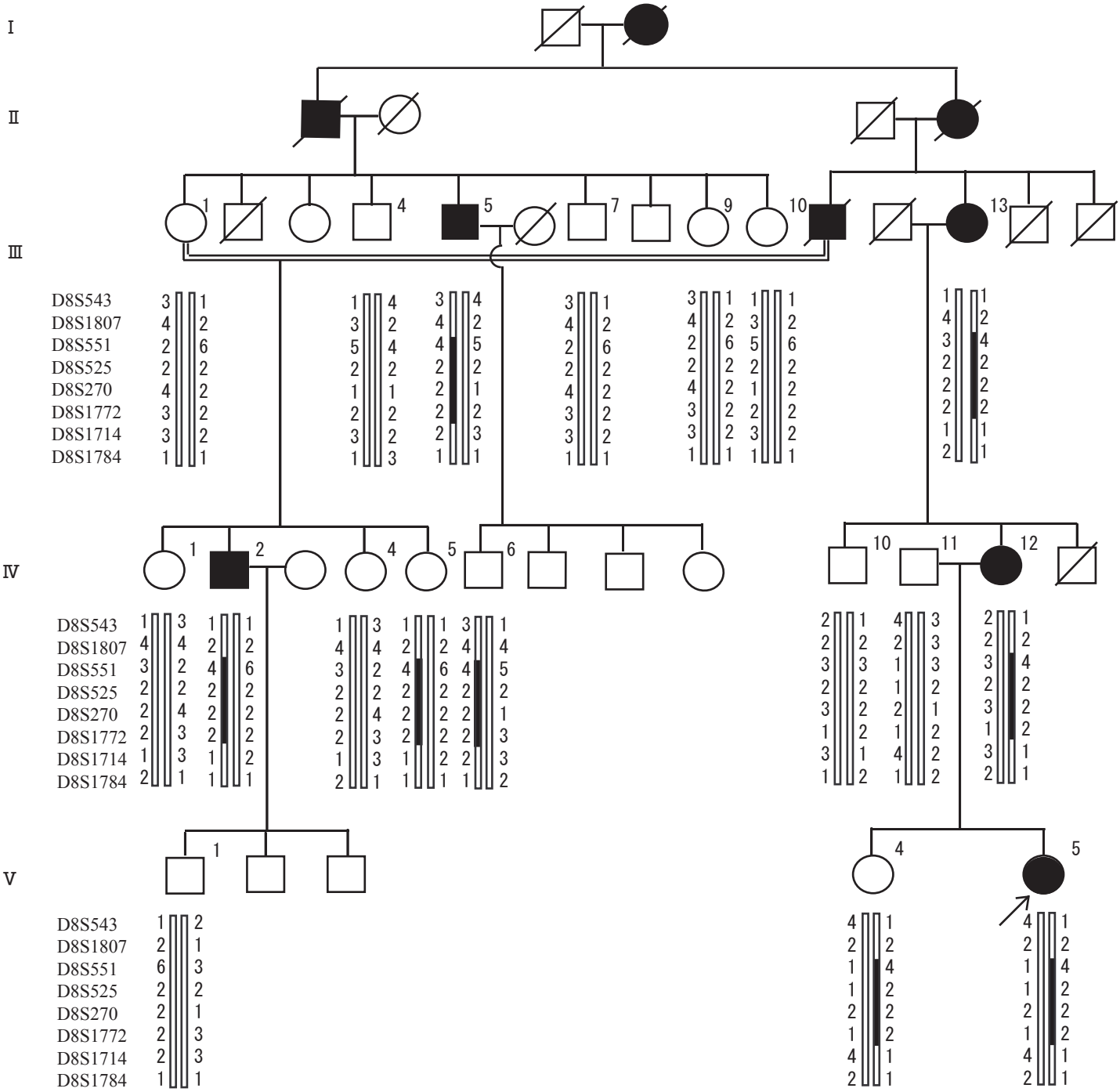
I
II
III
IV
V
D8S543
D8S1807
D8S551
D8S525
D8S270
D8S1772
D8S1714
D8S1784

Figure 1B

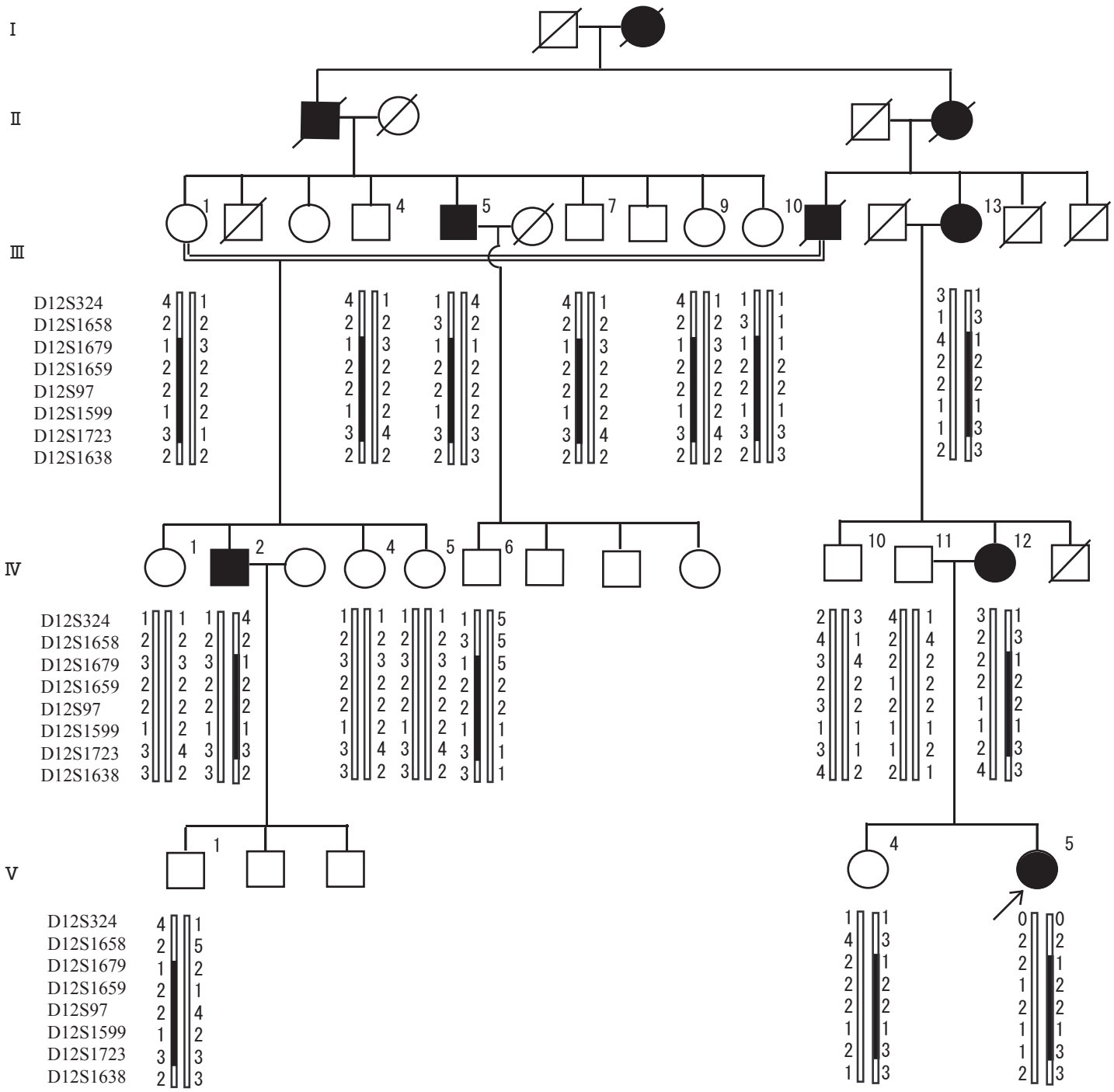
I
II
III
IV
V
D12S324
D12S1658
D12S1679
D12S1659
D12S97
D12S1599
D12S1723
D12S1638

Figure 1C

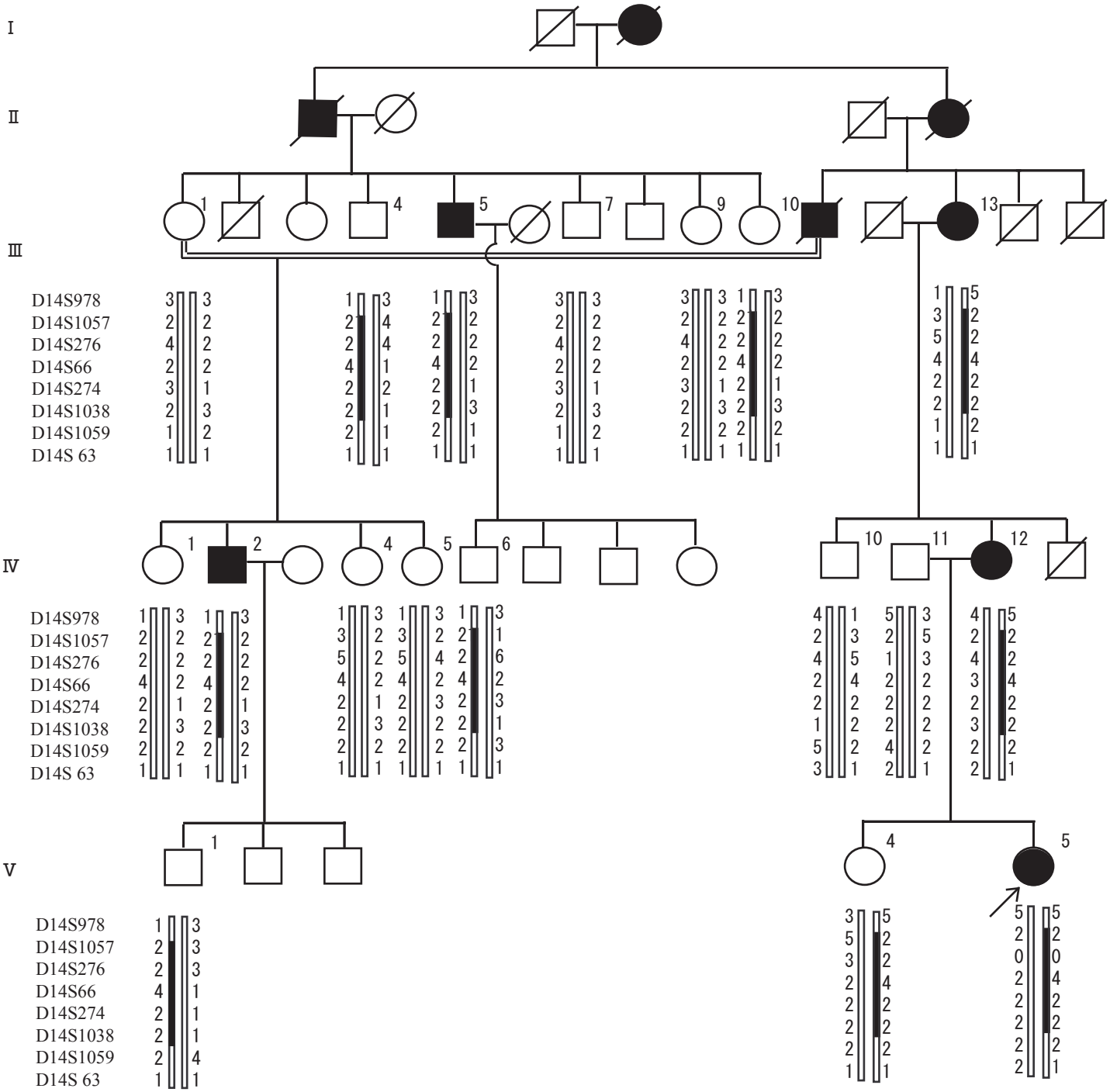
I
II
III
IV
V
D14S978
D14S1057
D14S276
D14S66
D14S274
D14S1038
D14S1059
D14S 63

Figure 3

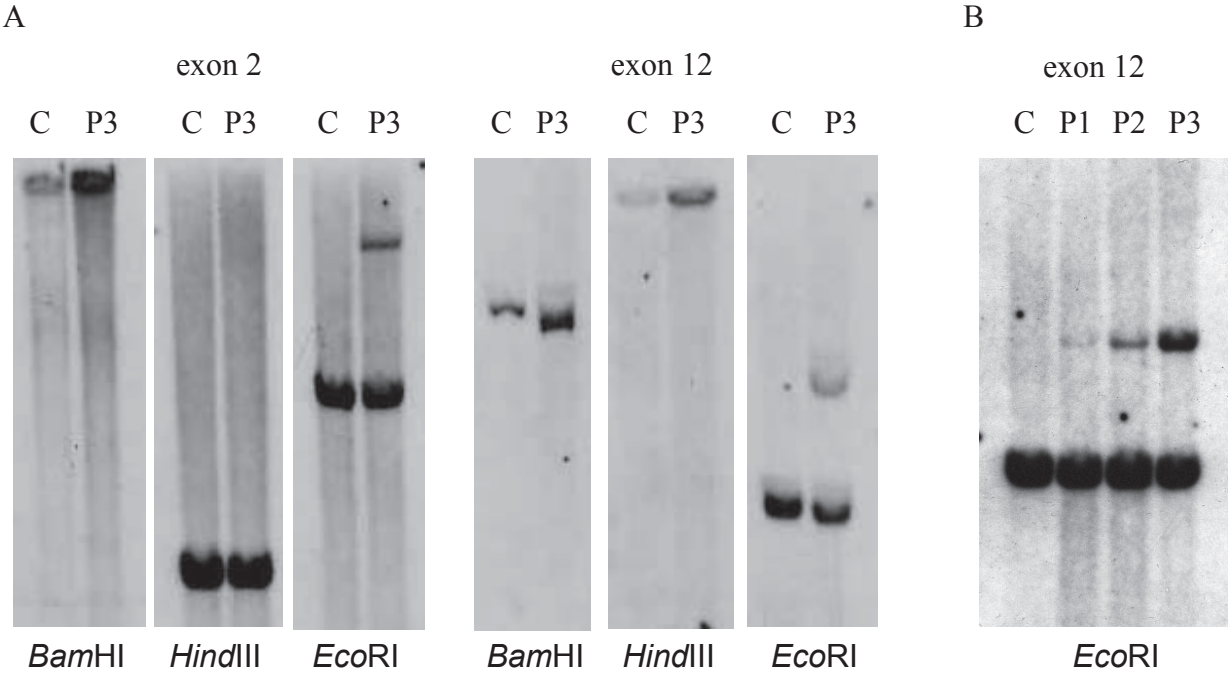
A
exon 2
C P3 C P3 C P3
BamHI HindIII EcoRI
exon 12
C P3 C P3 C P3
BamHI HindIII EcoRI
B
exon 12
C P1 P2 P3
EcoRI